Ecotoxicology and Environmental Safety 260 (2023) 115076

Contents lists available at ScienceDirect

Ecotoxicology and Environmental Safety

journal homepage: www.elsevier.com/locate/ecoenv

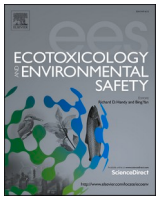

Cadmium inhibits powdery mildew colonization and reconstructs microbial community in leaves of the hyperaccumulator plant *Sedum alfredii*

Lingling Xu [a], Runze Wang [a], Bingjie Jin [a], Jiuzhou Chen [a], Tianchi Jiang [a], Waqar Ali [c], Shengke Tian [a,b], Lingli Lu [a,b,*]

[a] MOE Key Laboratory of Environment Remediation and Ecological Health, College of Environmental and Resource Sciences, Zhejiang University, Hangzhou 310058, China

[b] Key Laboratory of Agricultural Resource and Environment of Zhejiang Province, College of Environmental and Resource Sciences, Zhejiang University, Hangzhou 310058, China

[c] State Key Laboratory of Environmental Geochemistry, Institute of Geochemistry, Chinese Academy of Science's, Guiyang 550081, China

ARTICLE INFO

Edited by Muhammad Zia-ur-Rehman

Keywords:
Phyllosphere
Sedum alfredii Hance
Cadmium
Powdery mildew
Phytoremediation

ABSTRACT

Understanding the influence of the heavy metal cadmium (Cd) on the phyllosphere microbiome of hyperaccumulator plants is crucial for enhancing phytoremediation. The characteristics of the phyllosphere of *Sedum alfredii* Hance, a hyperaccumulator plant, were investigated using 16S rRNA and internal transcribed spacer amplicon sequencing of powdery mildew-infected leaves treated or untreated with Cd. The results showed that the colonization of powdery mildew caused severe chlorosis and necrosis in *S. alfredii* leaves, and the relative abundance of *Leotiomycetes* in infected leaves increased dramatically and significantly decreased phyllosphere microbiome diversity. However, *S. alfredii* preferentially accumulated higher concentrations of Cd in the leaves of infected plants than in uninfected plants by powdery mildew, which in turn significantly inhibited powdery mildew colonization in leaves; the relative abundance of the fungal class *Leotiomycetes* in infected leaves decreased, and alpha and beta diversities of the phyllosphere microbiome significantly increased with Cd treatment in the infected plants. In addition, the inter-kingdom networks in the microbiota of the infected leaves treated with Cd presented many nodes and edges, and the highest inter-kingdom modularity compared to the untreated infected leaves, indicating a highly connected microbial community. These results suggest that Cd significantly inhibits powdery mildew colonization by altering the composition of the phyllosphere microbiome in *S. alfredii* leaves, paving the way for efficient heavy metal phytoremediation and providing a new perspective on defense strategies against heavy metals.

1. Introduction

Cadmium (Cd) is a widespread soil contaminant originating from both natural and anthropogenic sources (Wei and Yang, 2010; Zhao et al., 2015). The accumulation of Cd in the environment poses a threat to human health and ecosystems (Rubina et al., 2020; Zhang et al., 2014). Phytoremediation is a relatively new technology considered novel, feasible, eco-friendly, cost-efficient, solar-driven, and is applicable in situ with adequate community acceptance (Clemens et al., 2013; McGrath and Zhao, 2003). Translocation of metals to plant shoots is a crucial biochemical process required for active phytoextraction (Tangahu et al., 2011; Zacchini et al., 2009). Phytoremediation efficiency is largely determined by the storage capacity of the shoots; however, pathogen infections often affect plant mineral nutrient homeostasis (Zeng et al., 2022). As previously reported, *Glycine max* infected with a specialized fungus mobilizes local zinc (Zn) in the roots (Morina et al., 2021), and pathogen-infected Arabidopsis leaves may accumulate Zn at the infection site (Escudero et al., 2022). Furthermore, foliar diseases such as powdery mildew severely affect plant growth and the accumulation of heavy metals, thus seriously affecting

Abbreviations: ANOVA, analysis of variance; ASVs, amplicon sequence variants; DS, disease severity; iTOL, Interactive Tree Of Life; ND, not detected; OTU, operational taxonomic unit; PCoA, principal coordinate analysis; PM, *S. alfredii* infected with powdery mildew; PMCd, *S. alfredii* treated with 25 μmol L^{-1} Cd and infected with powdery mildew; and SD, standard deviation.

* Corresponding author at: College of Environmental & Resources Sciences, Zhejiang University, Hangzhou 310058, China.
E-mail address: lulingli@zju.edu.cn (L. Lu).

https://doi.org/10.1016/j.ecoenv.2023.115076
Received 9 February 2023; Received in revised form 27 April 2023; Accepted 24 May 2023
Available online 29 May 2023

phytoremediation efficiency (Zou et al., 2018). However, few studies have been devoted to understanding the relationship between heavy metals and microbiota, specifically the phyllosphere microbiota.

Being the aerial part of plants, the phyllosphere is the most ubiquitous and specific habitat for diverse microorganisms (Chen et al., 2018; Chen et al., 2020), and many microbes reside on leaf surfaces (Vorholt, 2012). The microbial community of the phyllosphere plays an important role in protecting plants from pathogens (Jia et al., 2018; Mejia et al., 2008), The phyllosphere microbiome interacts with the host plant and beneficially affects its health and function (Stone et al., 2018). There is growing evidence that plants experience biotic and abiotic stresses and require vigorous support from microbes to increase their ability to fight stress (Liu et al., 2020). In addition to disease protection, the phyllosphere microbiome can influence many other plant traits, including mineral nutrient homeostasis (Gong and Xin, 2021; Salas-Gonzalez et al., 2021; Zeng et al., 2022). These studies have also demonstrated the importance of microbial homeostasis on plant growth and health. However, whether and how the phyllosphere microbiome responds to heavy metals in hyperaccumulating plants remains unclear.

Over the past few decades, hyperaccumulator plants have attracted great interest because of their superior ability to transport and accumulate high concentrations of heavy metals in their aboveground parts without showing any phytotoxic effects (Krämer, 2010; Manara et al., 2020), which is valuable for their potential use in phytoremediation, especially in phytoextraction (Zhao and McGrath, 2009). *Sedum alfredii* Hance (*S. alfredii*) is native to China and is one of the few non-*Brassica* species that can hyperaccumulate Zn and Cd (Lu et al., 2008). Powdery mildew, a ubiquitous foliar disease, causes severe phytosanitary threats to *S. alfredii* growth, leading to a loss of quality and heavy metal phytoremediation if control measures are not implemented (Nerva et al., 2019). As one of the most toxic heavy metals, Cd is a potential line of defense against pathogens. Therefore, considering the relationship between Cd and powdery mildew infection, or the phyllosphere microbiome, can help devise better strategies to prevent pathogen infection, promote the accumulation of heavy metals in hyperaccumulator plants, and improve phytoremediation efficiency.

Therefore, this study aimed to (i) compare the differences in the phyllosphere microbiome of *S. alfredii* treated with or without Cd in response to powdery mildew infection and (ii) examine whether and how the Cd-regulated phyllosphere microbiome protects *S. alfredii* from pathogen infection. The results of this study provide additional evidence for phytoextraction.

2. Materials and methods

2.1. Plant materials and culture

Seeds of *Sedum alfredii* Hance, a Cd hyperaccumulator, were obtained from an old Pb/Zn mine in the Zhejiang Province, China (Yang et al., 2004). As previously reported (Lu et al., 2008), seedlings were grown in uncontaminated soil for several generations, and healthy and uniform shoots were selected and pre-cultured. The selected shoots were rooted in water for one week and treated with 1/4- and 1/2-strength nutrient solutions for three days. The nutrient solution was prepared as described by (Lu et al., 2008), consisting of 0.1 mmol L^{-1} KCl, 0.7 mmol L^{-1} K_2SO_4, 5 μmol L^{-1} $ZnSO_4$, 0.1 mmol L^{-1} KH_2PO_4, 0.01 μmol L^{-1} $(NH_4)_6Mo_7O_{24}$, 0.2 μmol L^{-1} $CuSO_4$, 0.5 mmol L^{-1} $MgSO_4$, 10 μmol L^{-1} H_3BO_3, 100 μmol L^{-1} Fe-EDTA, 2 mmol L^{-1} $Ca(NO_3)_2$, and 0.5 μmol L^{-1} $MnSO_4$ (HuShi, Shanghai, China). Plants were then cultured in a full-strength nutrient solution, continuously aerated, and refreshed every 3 d. The pH of the nutrient solution was adjusted daily using NaOH or HCl to maintain the pH at 5.5–5.8. Plant cultivation was performed in a growth chamber (LeDian, Shanghai, China) under 16 h light and 8 h dark conditions. Light intensity during the photoperiod was set at 350 μmol m^{-2} s^{-2}, day and night temperatures of 26 °C and 20 °C, respectively, and chamber humidity of 65 %.

2.2. Experimental design and sample collection

For inoculation, 6-week-old seedlings were placed in a separate humid chamber (LeDian, Shanghai, China) at 23 °C for 72 h. Freshly collected powdery mildew spores were applied with a fine paintbrush to the adaxial surface of the leaves of *S. alfredii* seedlings and re-inoculated every day for 7 d at the same time (9:00 AM in China). Healthy and uniform 6-week-old seedlings were sprayed with sterile water in separate growth chambers under the same exposure and treatment conditions. As reported previously (Huai et al., 2019), *S. alfredii* seedlings inoculated with powdery mildew over 7 d, and *S. alfredii* showing similar infection rates, were chosen for treatment with 0 or 25 μmol L^{-1} $CdCl_2$ (202908, Sigma, USA) in a growth nutrient solution in a growth chamber at 26 °C for another 7 d. Finally, fresh plant samples from different treatment groups were collected in 50 mL Falcon tubes, frozen in liquid nitrogen at −80 °C (Thermo Scientific TSX70086V, USA), and analyzed as described below.

2.3. Infection quantification and elemental determination

As previously reported (Hao et al., 2015), disease severity (DS) in leaves was determined to quantify the powdery mildew infection index, with certain modifications. The DS had six levels, namely, DS = 0; 1, 0 < DS ≤ 20 %; 2, 20 % < DS ≤ 50 %; 3, 50% < DS ≤ 70 %; 4, 70 % < DS ≤ 90 %; 5, full susceptibility, DS ≥ 90 %; 6.

As previously reported (Hou et al., 2017; Tian et al., 2011), the *S. alfredii* seedlings were separated into roots, stems, and leaves immersed in 1.0 mmol L^{-1} EDTA for 5 min to remove surface-absorbed ions, and immediately rinsed thoroughly with distilled water for elemental determination. All samples were dried in an oven at 65 °C for 72 h until a constant weight was reached, after which the dry weight was measured. By using a graphite digestion instrument (GY-NDXJ, Yonggui, Shanghai), dried samples (0.1 g) of individual treatments were digested for 8 h at 180 °C with 1 mL H_2O_2 (1.0 mol L^{-1}) and 3 mL HNO_3 in a glass digestive tube with a glass funnel. The digested sample solution was transferred to a flask, and the volume was made up to 50 mL with highly purified deionized water and filtered for elemental determination. Inductively coupled plasma mass spectrometry (Agilent 7500a, USA) was used to determine the Cd concentrations in the digested sample solutions. We digested and analyzed a standard powder (rice powder, GBW08512, National Research Center for Certified Reference Materials of China) for quality control and assurance. Each treatment group consisted of 24 *S. alfredii* plants from eight pots, representing eight biological replicates.

2.4. Phyllosphere microbial DNA extraction

For microbial DNA extraction from the leaf phyllosphere, 10.0–15.0 g fresh leaf samples were collected from fresh *S. alfredii*, with 20 leaves per plant. Each harvested plants' leaves were stored in eight sterile bottles containing release buffer with 100.0 mL, 0.1 mol L^{-1}, and pH 8.0, and sterilized potassium phosphate buffer solution to uphold leaf integrity, as previously described (Bodenhausen et al., 2013; Ruiz-Perez et al., 2016; Xiong et al., 2021a, 2021b). The leaf samples were sonicated at 40 kHz for 1 min, and the solution was shaken at 180 rpm for 30 min at 24 °C, with the procedure repeated twice to ensure quality control and assurance. The plant tissues were removed using sterile tweezers, and the wash solution containing the microorganisms was filtered through a 0.22 μm nitrocellulose membrane filter (JinTeng, China). The filter membranes were then cut into pieces, and total microorganism DNA was extracted using the MP FastDNA® SPIN Kit for Soil (MP Biochemicals, Solon, OH, USA), following the manufacturer's instructions.

2.5. Generation of amplicons

The PCR cycling conditions included an initial denaturation of DNA

at 94 °C for 5 min, followed by 30 cycles of denaturation at 94 °C for 30 s, annealing at 52 °C for 30 s, and extension at 72 °C for 30 s, followed by a final extension at 72 °C for 10 min. The PCR products were mixed in equidensity ratios according to GeneTools Analysis Software (version 4.03.05.0, SynGene) and sequenced on an Illumina Nova6000 platform (New England Biolabs, MA, USA) by MeiGe Genomic Biotech (Guangzhou, China). Fragments of the bacterial 16 S rRNA (V4–V5) genes were amplified using primer sets 515 F:5′-GTGCCAGCMGCCGCGGTAA-3′ and 806 R:5′-CCGTCAATTCMTTTRAGTTT-3. ' In contrast, the fungal internal transcribed spacer (ITS) region containing the ITS1–2 genes was amplified using primer sets 1737 F:5′-CTTGGTCATTTAGAGGAAGTAA-3′ and 2043 R:5′-GCTGCGTTCTTCATCGATGC-3. ' The amplicons were sequenced on a MiSeq platform (Illumina, CA, USA).

2.6. Processing of pyrosequencing data

After MiSeq sequencing, the reads were analyzed using the Quantitative Insight into Microbial Ecology 2 (QIIME 2, version 2020.11) software and its plugins. DADA2 was then used to filter out noise and low-quality reads and eliminate chimeras to obtain amplicon sequence variants (ASVs) (Callahan et al., 2016). The ASVs of bacteria and fungi were assigned to taxonomic groupings based on comparisons with the SILVA 16S (version 12_8) (Quast et al., 2013) and UNITE ITS databases (version 7.0) (Koljalg et al., 2005), respectively. After classifying ASVs, bacterial ASVs were filtered and assigned to archaea, mitochondria, chloroplasts, and those that did not have a recognized kingdom assignment; the average frequency per sample was 11721.0. For fungal ASVs, plants and protists were removed and the average frequency per sample was 11779.3.

2.7. Statistical analysis

The functional diversity of taxonomic α- (Shannon diversity, Faith phylogenetic diversity (Faith_pd), and observed diversity) and α- (between samples) diversity indices were determined using QIIME 2. Cluster and principal coordinate analyses (PCoA) were performed based on Bray–Curtis dissimilarities across sequence samples. The results of these analyses were presented using the "PCoA" function of the "ape" package in the R software (version 4.2.0).

Manhattan plots were constructed using the edgeR package in R software utilizing operational taxonomic unit (OTU)-based approaches to evaluate the differential expression of OTU across the treatments based on $\log_2|\text{fold change}| \geq 2$ and Q-value > 0.05 (Robinson et al., 2010). A taxonomic dendrogram based on specific microbial clusters was generated with one representative sequence of each OTU using Mega-X (Kumar et al., 2016) and was displayed using the Interactive Tree Of Life (iTOL) (https://itol.embl.de/) (Letunic and Bork, 2011).

Molecular ecology networks of *S. alfredii* phyllosphere microbes based on the random matrix theory were constructed using molecular ecological network analyses (http://ieg4.rccc.ou.edu/mena) (Xiao et al., 2022). *P* values were adjusted using the "Benjamini–Hochberg" procedure (Benjamini and Hochberg, 1995) to reduce false-positive signals. The Gephi interactive platform (Bastian et al., 2009) was used to visualize molecular ecological networks. In microbiome networks, nodes represent individual microbial genera and edges represent the pairwise correlations between nodes, which indicate biologically or biochemically meaningful interactions.

The "Fungi" + "Functional" + "Guild" (FUNGUILD, version 1.0) was used to predict the functions of fungal taxa (Langille et al., 2013), respectively. A heat map was generated using the ggplot2 (version. 3.2.1) graphic system in the R package (Villanueva and Chen, 2019) to visualize the enrichment profile of each fungal function.

Statistical analysis of the elemental determination was performed using the IBM® SPSS® Statistics 25 (IBM, USA) application, and analysis of variance (ANOVA) was used on the data sets. The mean and standard deviation (SD) of individual treatments and the SD for each of the corresponding datasets ($P < 0.05$, $P < 0.01$) was calculated. The figures were created using OriginPro version 2021b software (OriginLab, Northampton, MA, USA) and the R package (version 4.2.0).

3. Results

3.1. Cd inhibits powdery mildew colonization in S. alfredii leaves

S. alfredii is highly sensitive to powdery mildew. After 7 d of powdery mildew exposure, the infected *S. alfredii* leaves developed symptoms of severe chlorosis and necrosis without Cd treatment (Fig. 1a). Meanwhile, the leaf biomass of infected *S. alfredii* significantly decreased by 0.70 g of fresh weight as the powdery mildew infection rate increased to 60.45 % (Fig. 1a, b, and d). However, in contrast to infected plants grown in a Cd-free nutrient solution, infected plants grown in a nutrient solution containing 25 μmol L^{-1} $CdCl_2$ showed a considerable decrease in the powdery mildew infection index, remaining at only 9.5 % (Fig. 1d), wherein the leaves remained green and leaf biomass increased to 4.27 g (Fig. 1a and b). The powdery mildew infection rate also had a significantly negative linear correlation with Cd treatment ($R^2 = 0.7056$, $P < 0.01$) (Fig. 1e), and the concentration of Cd in the aerial parts of *S. alfredii* increased 2-fold with powdery mildew infection (Fig. 1c).

3.2. Distinct microbiota community structure in the S. alfredii phyllosphere

Based on the Bray–Curtis distances, we further investigated the beta-diversity (β-diversity) of the overall variation in the microbiota community structure among samples in the *S. alfredii* phyllosphere across all treatments. Combined with cluster analysis, the PCoA of Bray–Curtis distances revealed that the phyllosphere fungal community in plants with powdery mildew infection formed separate clusters and was significantly separated from the other treatments across the first principal coordinate. However, the fungal community diversity of infected *S. alfredii* with Cd clustered with that of the uninfected plants (Fig. 2a). However, although the average distance of the Bray–Curtis matrix reached 0.92 with severe powdery mildew infection, Cd treatment significantly decreased the Bray–Curtis distance in the infected plants by 0.27, resulting in no significant difference between the Bray–Curtis distances in plants uninfected with powdery mildew and Cd-treated plants infected with powdery mildew (Fig. 2b). Thus, these results indicate that in the leaves of *S. alfredii* without Cd treatment, the fungal communities were more susceptible to powdery mildew than in the plants treated with Cd.

Furthermore, FUNGuild was used to annotate fungal functions. The principal component analysis results also revealed that the functions of phyllosphere fungi in powdery mildew infection were significantly separated across the first principal coordinate (Fig. S1a), and the function of the plant pathogen reached 99.29 % (Fig. S1b). However, after Cd treatment, plant pathogen abundance decreased rapidly (33.85 %). The abundance of undefined saprotrophs (20.70 %) and animal pathogen-plant pathogen-undefined saprotrophs (19.43 %) increased (Fig. S1b).

3.3. Diversity and abundance of the phyllosphere fungal community

Next, we determined the phyllosphere microbiota composition in powdery mildew-infected *S. alfredii* plants subjected to Cd treatment (0 or 25 μmol L^{-1} $CdCl_2$) and in uninfected plants subjected to Cd treatment (0 or 25 μmol L^{-1} $CdCl_2$). There was a significant difference between the relative abundance of phyllosphere fungal taxa with and without Cd treatment under powdery mildew infection (Fig. 3). Uninfected with powdery mildew, *Dothideomycetes* (25.51 % in the control and 35.94 % in the Cd treatment), *Sordariomycetes* (10.53 % in the control and 14.30 % in the Cd treatment), *Basidiomycota* (30.17 % in the control and 14.25 % in the Cd treatment), and *Leotiomycetes* (9.76 % in

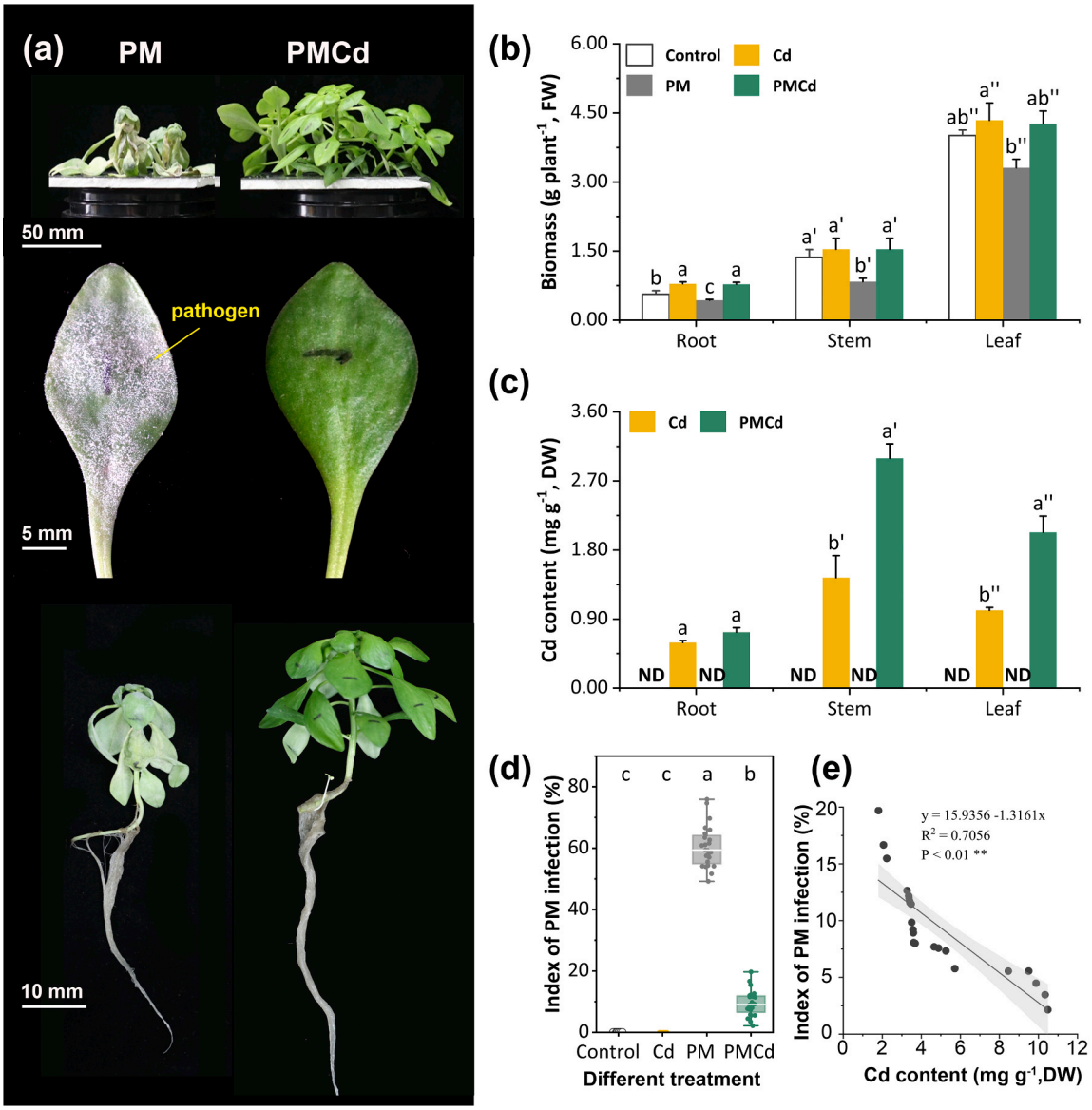

Fig. 1. The effect of Cd on powdery mildew colonization. Six-week-old seedlings were pre-treated with either powdery mildew (PM, PMCd) or with sterile water (control, Cd) for 7 d, then treated with 0 (control, PM) or 25 μmol L^{-1} $CdCl_2$ (Cd, PMCd) in nutrient solution at 26 °C for another 7 d. Images of *S. alfredii* plants and representative leaves infected by powdery mildew and treated with 0 μmol L^{-1} $CdCl_2$ (PM) or 25 μM $CdCl_2$ (PMCd) (a); Fresh-weight biomass of roots, stems, and leaves in the four treatment groups (control, Cd, PM, and PMCd) (b); Cd concentrations in mg g^{-1} dry weight biomass of roots, stems, and leaves of infected and uninfected plants treated with 25 μM $CdCl_2$ (Cd, PMCd) (c); Percentage of PM infection in leaves collected from *S. alfredii* subjected to different treatments (d); Correlation between Cd treatment and PM infection rate (e) Data represent mean ± SD (n = 8). Different letters indicate significant differences within different treatments ($P < 0.05$). Control, no powdery mildew with 0 μmol L^{-1} Cd treatment; Cd, no powdery mildew with 25 μmol L^{-1} Cd treatment; PM, powdery mildew infection with 0 μmol L^{-1} Cd treatment; and PMCd, powdery mildew infection with 25 μmol L^{-1} Cd treatment.

the control and 9.54 % in the Cd treatment) were the most dominant fungal classes in the leaves of *S. alfredii* (Fig. 3a). However, the relative abundance of *Leotiomycetes*, which is responsible for powdery mildew disease, increased significantly to 99 % with powdery mildew infection in the control group. In contrast, for *S. alfredii* treated with 25 μmol L^{-1} $CdCl_2$ after exposure to powdery mildew infection, the relative abundance of *Leotiomycetes* decreased significantly to 43.7 %. The relative abundances of other classes, such as *Dothideomycetes* (10.42 %), *Sordariomycetes* (3.70 %), and *Basidiomycota* (38.00 %), significantly increased in the leaves of *S. alfredii* exposed to powdery mildew and subjected to Cd treatment (Fig. 3a).

A three-way ANOVA, including Shannon, Faith-pd, and observed OTU diversity, revealed that the alpha diversity (α-diversity) (within-sample diversity) of the fungal communities in *S. alfredii* (Shannon index $_{[PM]} = 0.28$, $P < 0.01$; Faith_pd$_{[PM]} = 10.36$, $P < 0.01$; and observed OTU diversity$_{[PM]} = 90.63$, $P < 0.01$) (Fig. 3b, c, and d) was sharply decreased without Cd treatment under powdery mildew infection condition. However, with the 25 μmol L^{-1} Cd treatment, the fungal community diversity of powdery mildew-infected *S. alfredii* significantly increased (Shannon index $_{[PMCd]} = 3.04$, 10.97-fold of PM treatment; Faith_pd$_{[PMCd]} = 17.87$, 1.72-fold of PM treatment; and observed OTU diversity$_{[PMCd]} = 190.75$, 2.10-fold of PM treatment) (Fig. 3b, c, and d). In contrast, there was no significant difference in the composition of total leaf bacteria in *S. alfredii* among any of the treatments (control, Cd, PM, and PMCd) (Fig. S2).

3.4. Phyllosphere fungal assemblage divergence between S. alfredii infected and healthy leaves

A comparison of fungal assemblages in the leaves of *S. alfredii* with

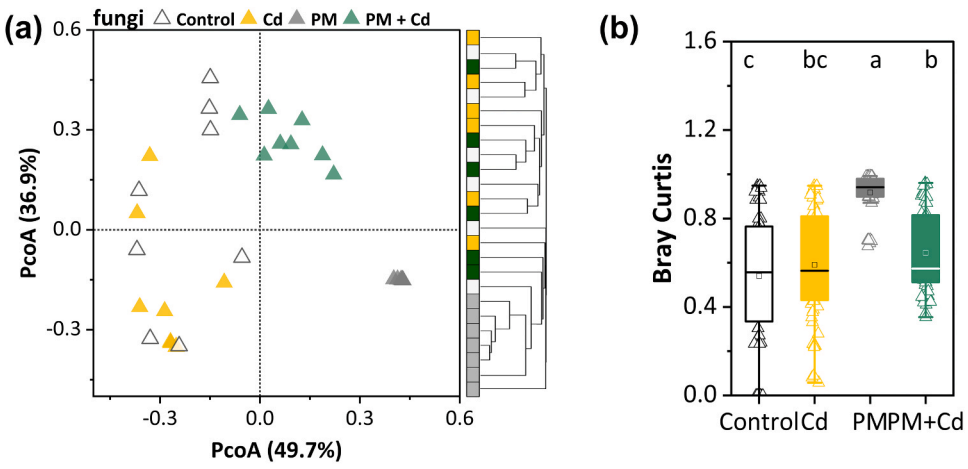

Fig. 2. The phyllosphere microbiome community structure in *S. alfredii* populations. Six-week-old seedlings were pre-treated with either powdery mildew (PM, PMCd) or with sterile water (control, Cd) for 7 d, then treated with 0 (control, PM) or 25 μmol L^{-1} $CdCl_2$ (Cd, PMCd) in nutrient solution at 26 °C for another 7 d. Principal coordinate analysis (PCoA) plots were used to show Bray–Curtis distances among the fungal communities compared with the hierarchical clustering of measurable OTUs (operational taxonomic units), based on pairwise Bray–Curtis similarity (a); Bray–Curtis distances among the phyllosphere microbiome in control, Cd, PM, and PMCd in *S. alfredii* leaves (b). Data represent mean ± SD (n = 8). Different letters indicate significant differences within different treatments ($P < 0.05$). Control, no powdery mildew with 0 μmol L^{-1} Cd treatment; Cd, no powdery mildew with 25 μmol L^{-1} Cd treatment; PM, powdery mildew infection with 0 μmol L^{-1} Cd treatment; PMCd, powdery mildew infection with 25 μmol L^{-1} Cd treatment; SD, standard deviation.

and without exposure to powdery mildew infection revealed that *Dothideomycetes*, *Exobasidiomycetes*, *Sordariomycetes*, and *Ustilaginomycetes* were abundant in the leaves of *S. alfredii* in the Control, Cd, and PMCd treatments. In contrast, *Leotiomycetes* were severely enriched in the infected leaves of *S. alfredii* without Cd treatment (Fig. 4a). As shown in the Venn diagram (Fig. 4b), 13 fungal taxa that were shared among the Control, Cd, and PMCd treatments belonged to *Dothideomycetes*, *Sordariomycetes*, and *Ustilaginomycetes* classes. Fig. 4c shows that *Dothideomycetes*, *Sordariomycetes*, and *Ustilaginomycetes* were abundant in uninfected and infected leaves subjected to Cd treatment, and the abundance of *Ustilaginomycetes* significantly increased in infected leaves subjected to Cd treatment. However, in the infected *S. alfredii* leaves, *Leotiomycetes* were enriched, and other fungal taxa were significantly less abundant (Fig. 4a, c, and d). Furthermore, based on the phylogenetic tree and relative abundances of these OTUs displayed in Fig. 4d, it is clear that PM-enriched *Leotiomycetes* are closely related to *Dothideomycetes*. However, the relationships among *Leotiomycetes*, *Exobasidiomycetes* and *Ustilaginomycetes* remain unclear.

3.5. Changes in phyllosphere microbiota co-occurrence networks

To further investigate whether the variations in microbial interactions accompanied variations in microbial community assemblies, we analyzed the fungal–fungal intra-kingdom networks and bacterial–fungal inter-kingdom networks to uncover possible associations and the complexity of connections among the phyllosphere microbiota. Based on the co-occurrence network analysis of the fungal–fungal and bacterial–fungal networks, the highest number of nodes and edges with the Cd treatment (nodes: 207, edges: 2530 in intra-kingdom and nodes: 216, edges: 1256 in inter-kingdom network analysis; Fig. 5, Table S1) was observed. Furthermore, the intra-kingdom and inter-kingdom networks in infected leaves subjected to Cd treatment were more complex (based on the number of nodes and edges) than those in infected leaves without Cd treatment, with the highest intra-kingdom complexity (average degree = 38.94) and highest inter-kingdom modularity (modularity = 0.66). However, in the powdery mildew-infected leaves, the network presented the lowest number of nodes and the highest number of negative edges (nodes: 60, proportion of negative edges 47.11 % in intra-kingdom and 161/46.34 % in inter-kingdom with 63.16 % in bacterial–fungal, Fig. 5a–e, Table S1). Finally, co-enriched OTUs (between all uninfected and infected leaves subjected to the Cd treatment) were also found, as shown in Fig. 4, and were highly connected to other fungi in the intra-kingdom networks (Fig. 5a). Compared to infected leaves, the nodal degree of these co-enriched OTUs increased significantly in infected leaves subjected to Cd treatment (Fig. 5a, b; Table S2). The powdery mildew node degree (of *Leotiomycetes*) reached 31 in the infected leaves, but significantly decreased to 2 in the CD treated infected leaves (Table S2).

4. Discussion

The phyllosphere microbiome is ubiquitous in the aerial parts of plants and is essential for plant growth and disease resistance (Vorholt, 2012). In the current study, by profiling the differences in the phyllosphere microbiome among the infected and uninfected *S. alfredii* leaves with or without 25 μM Cd treatment, we found that Cd application might significantly influence powdery mildew colonization, maintain phyllosphere microbiome diversity, and help *S. alfredii* recruit other microbiome taxa to cope with powdery mildew infection. *S. alfredii* can thrive, accumulate large amounts of Cd in its aboveground parts, and improve the phytoremediation efficiency of Cd-polluted soils (Tian et al., 2017).

4.1. Cd efficiently inhibited powdery mildew colonization in S. alfredii

As a biotrophic fungus, powdery mildew severely influences *S. alfredii* growth and affects the Cd concentration balance (Fig. 1). As an important hyperaccumulator plant, *S. alfredii* has a strong ability to hyperaccumulate heavy metals such as Zn and Cd in its aerial parts (Deng et al., 2007; Yang et al., 2004). The results obtained in this study showed that powdery mildew-infected *S. alfredii* exhibited enhanced Cd accumulation in shoots, which may decrease the nutrient status in leaves and cause powdery mildew to suffer high Cd toxicity while obtaining nutrients, and thus may strongly restrict powdery mildew acquisition and, therefore, their growth (Fig. 1a). Similarly, our results are consistent with previous results showing that *Brassica juncea* can accumulate selenium to protect Indian mustard plants from fungal infection and herbivory by caterpillars (Hanson et al., 2003), and that nickel hyperaccumulation in *Streptanthus polygaloides* enhances plant resistance to powdery mildew infection and bacterial pathogens (Boyd et al., 1994). Most studies have focused on the relationship between heavy metals and plant metabolism. However, the biological roles of Cd in the phyllosphere microbiome of the hyperaccumulator *S. alfredii* leaves have seldom been reported.

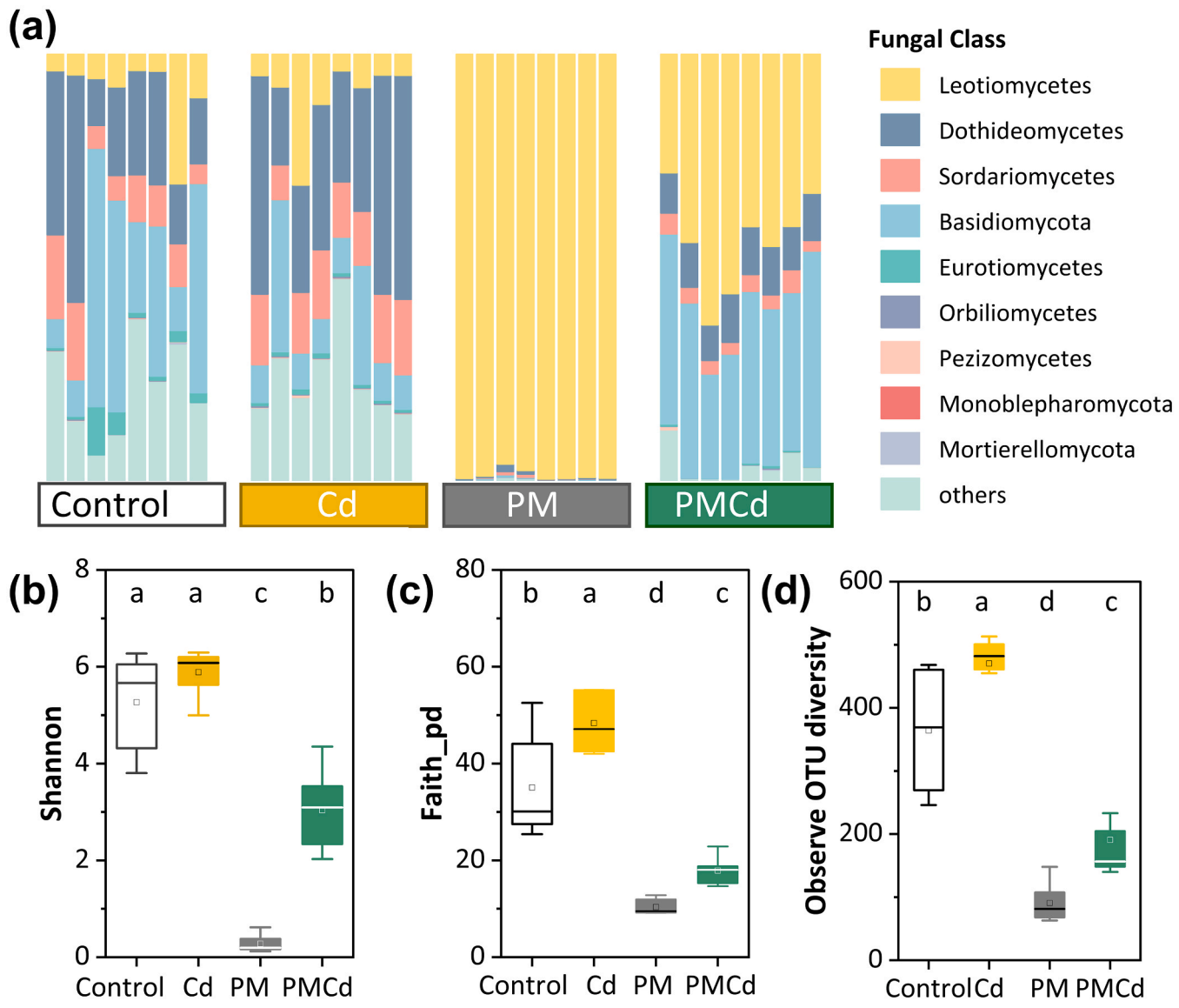

Fig. 3. Distribution of phyllosphere microbiome communities. Six-week-old seedlings were pre-treated with either powdery mildew (PM, PMCd) or with sterile water (control, Cd) for 7 d, then treated with 0 (control, PM) or 25 μmol L^{-1} $CdCl_2$ (Cd, PMCd) in nutrient solution at 26 ℃ for another 7 d. Relative abundances of different fungal classes in the phyllosphere microbiota of *S. alfredii* leaves (a); Shannon indices of the diversity of fungal classes (b); Faith phylogenetic distance (Faith_pd) of fungal classes (c); Observed OTU diversity of fungal classes (d). Data represent mean ± SD (n = 8). Different letters indicate significant differences within different treatments ($P < 0.05$). Control, no powdery mildew with 0 μmol L^{-1} Cd treatment; Cd, no powdery mildew with 25 μmol L^{-1} Cd treatment; PM, powdery mildew infection with 0 μmol L^{-1} Cd treatment; PMCd, powdery mildew infection with 25 μmol L^{-1} Cd treatment; OTU, operational taxonomic units; SD, standard deviation.

4.2. Cd efficiently maintained the diversity of the phyllosphere microbiome community

In this study, as judged by the α- and β-diversities, the community structure of phyllosphere microbiota was sharply altered by powdery mildew invasion. Fungal diversity dramatically decreases with powdery mildew infection. However, powdery mildew-infected *S. alfredii* treated with Cd efficiently inhibited powdery mildew colonization, reduced the dissimilarity of the fungal community, and was attributed to an increase in phyllosphere microbiome α-diversity (Figs. 2 and 3). A previous study found that high microbial diversity supports mutualistic microbial interactions that prevent pathobionts (Bodenhausen et al., 2014). The results of functional diversity investigations of phyllosphere fungi also support this view (Fig. S1). However, pathogen-infected plants may harbor altered leaf microbial communities (Humphrey and Whiteman, 2020), less diverse microbial communities, and may induce phyllosphere dysbiosis, and disease symptoms (Chen et al., 2020). However, perhaps because of coevolutionary processes, the phyllosphere microbial species on *S. alfredii* leaves may have evolved the ability to tolerate Cd toxicity. Meantime, as described previously, heavy metals can alter the composition of soil microbial communities (Wood et al., 2016). Furthermore, Cd treatment can be implicated in the assemblage of unique rhizosphere bacterial communities (Hou et al., 2017), and can change the structure and activity of indigenous microbial communities (Khan et al., 2010). Multiple functions associated with microbial metabolism are enriched in infected leaves subjected to Cd treatment, which may impart important benefits to the nutrition, health, and quality of the plants (Igiehon and Babalola, 2017; Nie et al., 2018). Consistent with these results, the decreasing divergence of fungal community assemblages during Cd treatment between infected and uninfected *S. alfredii* further indicates interactions between the phyllosphere system and Cd treatment. These results strongly indicate that

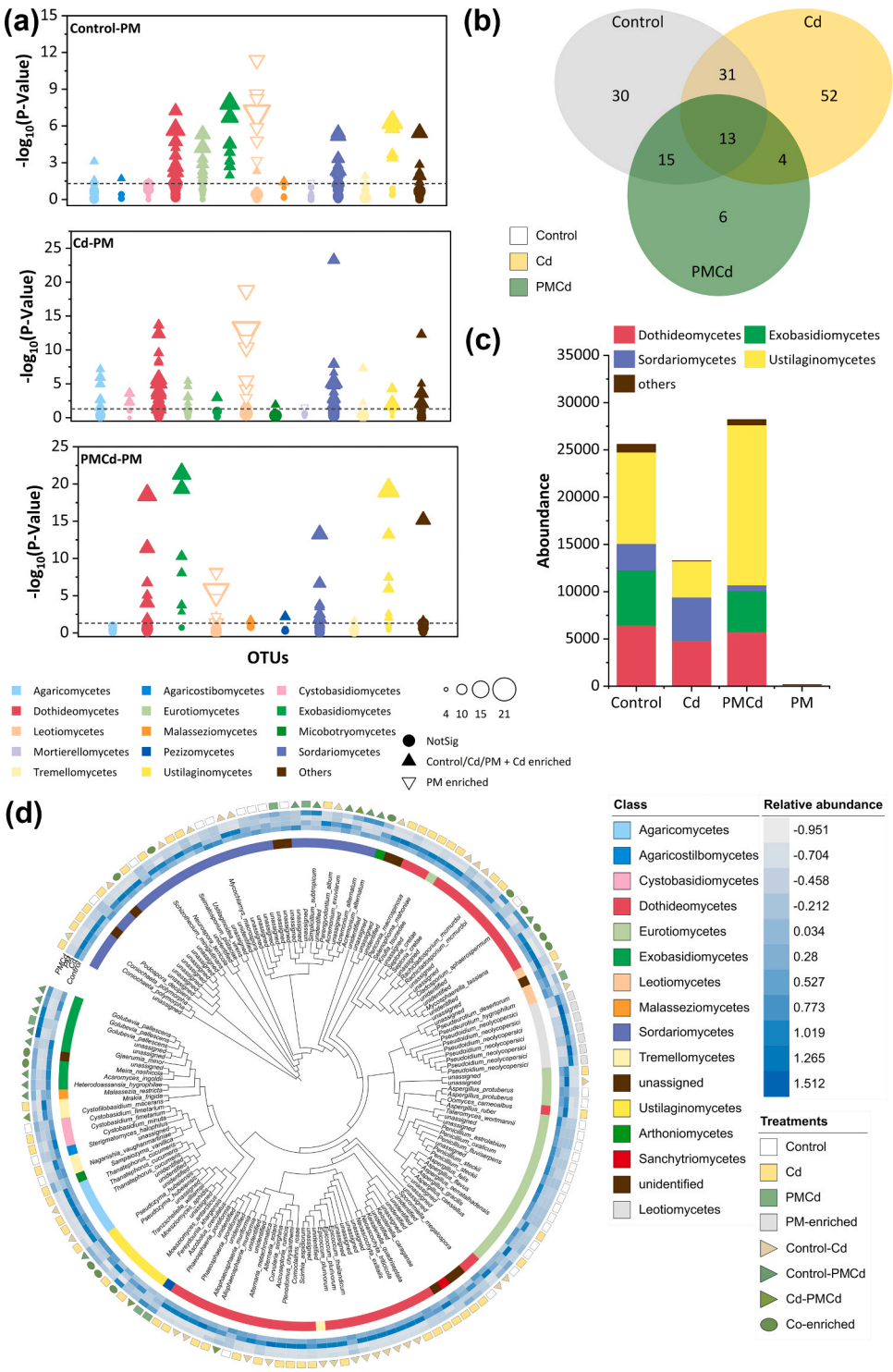

Fig. 4. Taxonomic characteristics of *S. alfredii* phyllosphere microbiome. Six-week-old seedlings were pre-treated with either powdery mildew (PM, PMCd) or with sterile water (control, Cd) for 7 d, then treated with 0 (control, PM) or 25 μmol L^{-1} $CdCl_2$ (Cd, PMCd) in nutrient solution at 26 ℃ for another 7 d. Manhattan plots present the differences in the relative abundance of enriched OTUs (operational taxonomic units) in the fungal populations in the *S. alfredii* phyllosphere between control versus PM, Cd versus PM, and PMCd versus PM (a); Venn diagram showing the overlap in the fungal classes among control, Cd, and PMCd treatments (b), which correspond to the information presented in the Manhattan plots shown in panel (a) ($P < 0.05$); Column chart presenting the relative abundance of the enriched OTUs in fungal classes at the phylum level (c) selected from the Venn diagram presented in panel (b); Taxonomic dendrogram showing the relative abundance of the enriched OTUs in fungal classes (d), corresponding to the overlap among control, Cd, and PMCd treatments evident in the Venn diagram shown in panel (b). Significantly enriched OTUs are depicted above the dashed line, corresponding to $P = 0.05$. Each circle or triangle represents a single OTU at the class level). OTUs enriched or depleted in the control, Cd, or PMCd treatments are represented by a filled triangle and an empty triangle, representing the PMCd treatment group. The sizes of the triangles correspond to their relative abundance in the respective samples. The taxonomic tree was constructed based on fungal ITS sequences. Control, no powdery mildew with 0 μmol L^{-1} Cd treatment; Cd, no powdery mildew with 25 μmol L^{-1} Cd treatment; PM, powdery mildew infection with 0 μmol L^{-1} Cd treatment; PMCd, powdery mildew infection with 25 μmol L^{-1} Cd treatment; ITS, internal transcribed spacer.

microbiome structure is crucial for plant health and metal hyperaccumulation. The results also showed that microbial diversity is strongly linked to powdery mildew resistance, and Cd efficiently maintains phyllosphere microbiome community diversity.

4.3. Cd increased the complexity of phyllosphere microbiota co-occurrence networks

Cooperative and competitive interactions between microbial species and network modularity can affect community stability (Coyte et al., 2015; Faust and Raes, 2012; Gao et al., 2021). In our study, the lowest modularity and highest proportion of negative correlations among fungal taxa were observed in powdery mildew-infected *S. alfredii* networks compared to those of the uninfected or Cd-treated *S. alfredii* networks (Fig. 5, Table S1). Mutually negative interactions indicated solid ecological competition, which also indicated that a lower variety of taxa could be hosted in infected *S. alfredii* leaves than in uninfected or Cd-treated *S. alfredii* leaves. In addition, lower modularity in the fungal network may exacerbate the destabilizing effect owing to the higher occurrence of cross-module correlations between taxa (Grilli et al.,

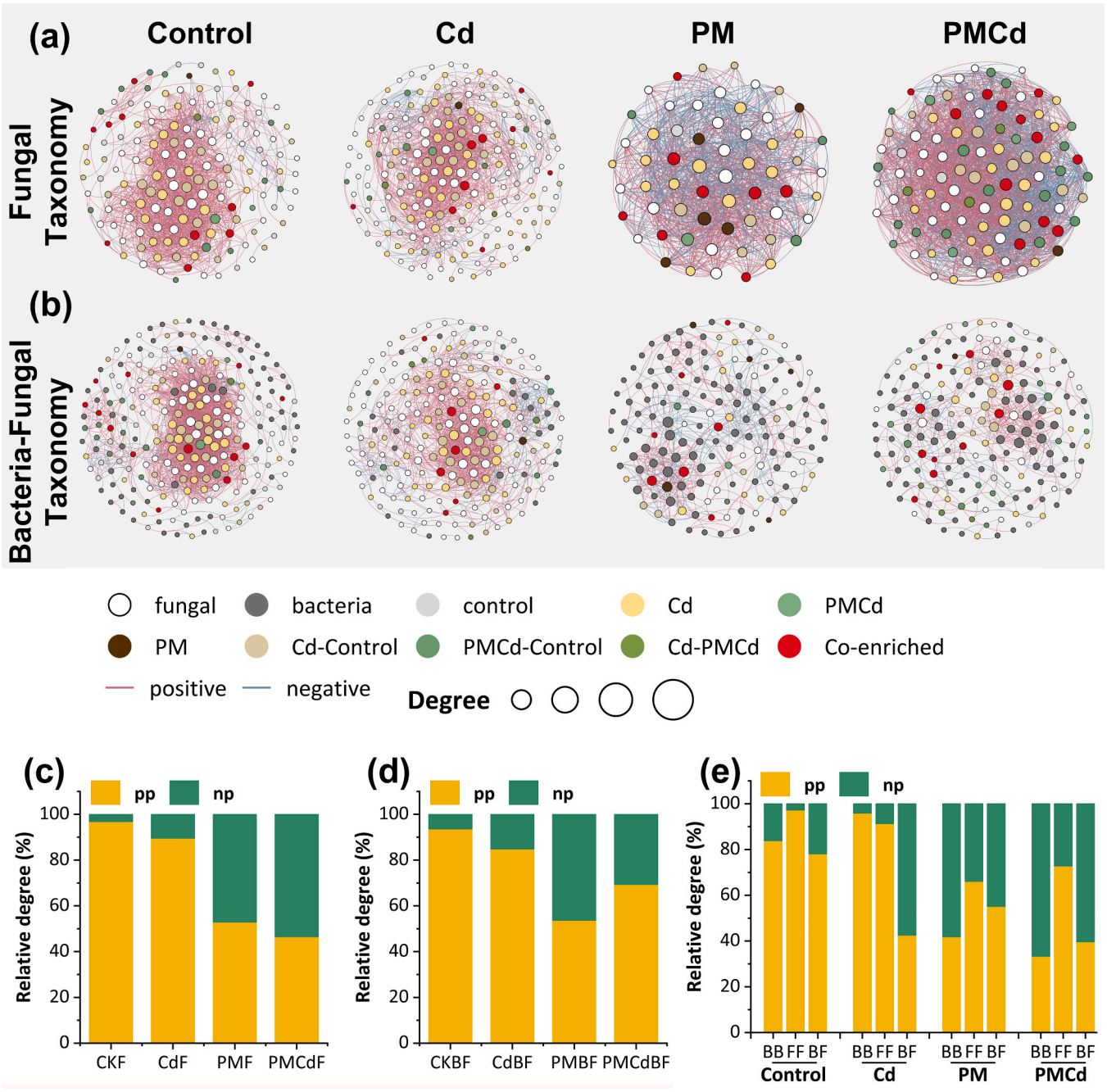

Fig. 5. The co-occurrence of networks among *S. alfredii* phyllosphere microbiome kingdoms. Six-week-old seedlings were pre-treated with either powdery mildew (PM, PMCd) or with sterile water (control, Cd) for 7 d, then treated with 0 (control, PM) or 25 μmol L^{-1} $CdCl_2$ (Cd, PMCd) in nutrient solution at 26 ℃ for another 7 d. Intra-kingdom (a) and inter-kingdom (b) co-occurrence of networks in the *S. alfredii* phyllosphere microbiome. The nodes are colored based on different treatments. Node size indicates the degree of connection between OTUs. Edge color represents positive (red) and negative (blue) correlations; the degree and interaction type in the fungal intra-kingdom networks (c), bacterial-fungal inter-kingdom networks (d), and the specific degree and interaction type of BB, FF, and BF networks (e) in each treatment group. Control, no powdery mildew with 0 μmol L^{-1} Cd treatment; Cd, no powdery mildew with 25 μmol L^{-1} Cd treatment; PM, powdery mildew infection with 0 μmol L^{-1} Cd treatment; PMCd, powdery mildew infection with 25 μmol L^{-1} Cd treatment; B, bacterial; F, fungal; BB, bacterial-bacterial; FF, fungal-fungal; BF, bacterial-fungal networks; pp, positive; np negative.

2016; Hernandez et al., 2021). The nodes and modularity among microbes in infected *S. alfredii* leaves significantly increased with Cd treatment (Fig. 5, Table S1), which is consistent with the results of many previous studies (Shi et al., 2020; Toju et al., 2018; Wagg et al., 2019). Based on its high modularity, *S. alfredii* efficiently enhanced inter- and intra-phyllosphere microbiome interactions, especially negative ones (Fig. 5, Table S1). Enhanced interactions improve network and hub taxa complexity, improve microbiome stability by diminishing the disrupting effects of cooperation (Coyte et al., 2015), enhance resistance to external stress (Wagg et al., 2019) and are important in supporting ecosystem functions.

4.4. Crucial microbiome assembled by S. alfredii leaves under Cd treatment

The phyllosphere of *S. alfredii* is characterized by a unique microbial community. The abundance of many fungi (at the OTU level) was higher in infected leaves subjected to Cd treatment than in infected leaves not

subjected to Cd treatment (Fig. 4). *Dothideomycetes*, *Sordariomycetes*, and *Ustilaginonmycetes* were widely present in uninfected or infected leaves subjected to Cd treatment and were less abundant in powdery mildew-infected samples (Fig. 4). These fungal taxa may confer new microbial functions to native microbiota in response to powdery mildew invasion. Emerging evidence has confirmed that several microbes recruited following stress may exhibit antagonistic activity against pathogens and benefit plant survival (Li et al., 2022). The results of the phylogenetic tree and network analysis in Fig. 4d and Fig. 5 show that the relationship between PM-enriched *Leotiomycetes*, Cd-enriched *Exobasidiomycetes*, and *Ustilaginomycetes* remains distant, suggesting that *Exobasidiomycetes* could have contributed to the suppression of powdery mildew via either resource or interference competition. For instance, *Arabidopsis thaliana* recruits a group of disease-resistance-inducing and growth-promoting beneficial microbes to downy mildew pathogen *Hyaloperonospora arabidopsidis* infection (Berendsen et al., 2018). Other studies have shown that *S. alfredii* recruits rhizobacteria to promote plant growth and improve phytoextraction (Hou et al., 2017; Wang et al., 2020).

5. Conclusions

Based on the presented data, our results demonstrate that phyllosphere fungal communities are sensitive to powdery mildew infection. However, Cd treatment efficiently inhibited *S. alfredii* powdery mildew infection, exerted a substantial effect on *S. alfredii* phyllosphere microbiome assembly, and may recruit other microbiome taxa to provide protection to host plants. Furthermore, phyllosphere homeostasis may promote *S. alfredii* to thrive efficiently and accumulate predominantly, thereby increasing Cd absorption and accumulation. Consequently, the current study significantly improves our understanding of the role of Cd in pathogen defense in the phyllosphere and the beneficial effects of Cd on phyllosphere microbiome assembly in the hyperaccumulator *S. alfredii* plants, which, in turn, could improve the performance of natural ecosystems and heavy metal phytoremediation.

Funding

This work was supported by the National Natural Science Foundation of China (grant numbers 22276164 and 41977130) and Natural Science Foundation of Zhejiang Province (grant number LZ22C150004).

CRediT authorship contribution statement

Lingling Xu: Collection, visualization, data analysis, software, writing - original draft preparation, writing- manuscript review. **Runze Wang**: Visualization, data curation, writing - reviewing and editing. JZC, BJJ, and TCJ: Data curation and visualization. Waqar Ali: Writing-reviewing and editing. **Lingli Lu** and **Shengke Tian**: Supervision, funding acquisition, and reagent provision. All authors discussed the results, reviewed and approved the final manuscript.

Declaration of Competing Interest

The authors declare that they have no known competing financial interests or personal relationships that could have appeared to influence the work reported in this paper.

Data Availability

Supplementary Information files. Raw RNA-seq data were deposited in the NCBI Sequence Read Archive (SRA) database under BioProject PRJNA868537 (http://www.ncbi.nlm.nih.gov/bioproject/868537).

Acknowledgments

The authors would also like to thank Editage (www.editage.cn) for the English language editing.

Appendix A. Supporting information

Supplementary data associated with this article can be found in the online version at doi:10.1016/j.ecoenv.2023.115076.

References

Bastian, M., Heymann, S., Jacomy, M., 2009. Gephi: an open source software for exploring and manipulating networks. Proc. Int. AAAI Conf. Web Soc. Media 361–362.
Benjamini, Y., Hochberg, Y., 1995. Controlling the false discovery rate - a practical and powerful approach to multiple testing. J. R. Stat. Soc. Ser. B-Stat. Methodol. 57 (1), 289–300.
Bodenhausen, N., Horton, M.W., Bergelson, J., 2013. Bacterial communities associated with the leaves and the roots of Arabidopsis thaliana. Plos One 8 (2), e56329.
Bodenhausen, N., Bortfeld-Miller, M., Ackermann, M., Vorholt, J.A., 2014. A synthetic community approach reveals plant genotypes affecting the phyllosphere microbiota. Plos Genet. 10 (4), e1004283.
Boyd, R.S., Shaw, J.J., Martens, S.N., 1994. Nickel hyperaccumulation defends Streptanthus polygaloides (brassicaceae) against pathogens. Am. J. Bot. 81 (3), 294–300.
Callahan, B.J., McMurdie, P.J., Rosen, M.J., Han, A.W., Johnson, A.J.A., Holmes, S.P., 2016. DADA2: high-resolution sample inference from Illumina amplicon data. Nat. Methods 13 (7), 581–583.
Chen, Q.-L., An, X.-L., Zheng, B.-X., Ma, Y.-B., Su, J.-Q., 2018. Long-term organic fertilization increased antibiotic resistome in phyllosphere of maize. Sci. Total Environ. 645, 1230–1237.
Chen, T., Nomura, K., Wang, X.L., Sohrabi, R., Xu, J., Yao, L.Y., Paasch, B.C., Ma, L., Kremer, J., Cheng, Y.T., et al., 2020. A plant genetic network for preventing dysbiosis in the phyllosphere. Nature 580 (7805), 653–657.
Clemens, S., Aarts, M.G.M., Thomine, S., Verbruggen, N., 2013. Plant science: the key to preventing slow cadmium poisoning. Trends Plant Sci. 18 (2), 92–99.
Coyte, K.Z., Schluter, J., Foster, K.R., 2015. The ecology of the microbiome: networks, competition, and stability. Science 350 (6261), 663–666.
Deng, D.M., Shu, W.S., Zhang, J., Zou, H.L., Lin, Z., Ye, Z.H., Wong, M.H., 2007. Zinc and cadmium accumulation and tolerance in populations of Sedum alfredii. Environ. Pollut. 147 (2), 381–386.
Escudero, V., Castro-Leon, A., Sanchez, D.F., Abreu, I., Bernal, M., Kramer, U., Grolimund, D., Gonzalez-Guerrero, M., Jorda, L., 2022. Arabidopsis thaliana Zn^{2+}-efflux ATPases HMA2 and HMA4 are required for resistance to the necrotrophic fungus Plectosphaerella cucumerina BMM. J. Exp. Bot. 73, 339–350.
Faust, K., Raes, J., 2012. Microbial interactions: from networks to models. Nat. Rev. Microbiol. 10 (8), 538–550.
Gao, M., Xiong, C., Gao, C., Tsui, C.K.M., Wang, M.M., Zhou, X., Zhang, A.M., Cai, L., 2021. Disease-induced changes in plant microbiome assembly and functional adaptation. Microbiome 9, 1–18.
Gong, T.Y., Xin, X.F., 2021. Phyllosphere microbiota: community dynamics and its interaction with plant hosts. J. Integr. Plant Biol. 63 (2), 297–304.
Grilli, J., Rogers, T., Allesina, S., 2016. Modularity and stability in ecological communities. Nat. Commun. 7 (1), 12031.
Hanson, B., Garifullina, G.F., Lindblom, S.D., Wangeline, A., Ackley, A., Kramer, K., Norton, A.P., Lawrence, C.B., Pilon-Smits, E.A.H., 2003. Selenium accumulation protects Brassica juncea from invertebrate herbivory and fungal infection. N. Phytol. 159 (2), 461–469.
Hao, Y., Parks, R., Cowger, C., Chen, Z., Wang, Y., Bland, D., Murphy, J.P., Guedira, M., Brown-Guedira, G., Johnson, J., 2015. Molecular characterization of a new powdery mildew resistance gene Pm54 in soft red winter wheat. Theor. Appl. Genet. 128 (3), 465–476.
Hernandez, D.J., David, A.S., Menges, E.S., Searcy, C.A., Afkhami, M.E., 2021. Environmental stress destabilizes microbial networks. Isme J. 15 (6), 1722–1734.
Hou, D.D., Wang, K., Liu, T., Wang, H.X., Lin, Z., Qian, J., Lu, L.L., Tian, S.K., 2017. Unique rhizosphere micro-characteristics facilitate phytoextraction of multiple metals in soil by the hyperaccumulating plant Sedum alfredii. Environ. Sci. Technol. 51 (10), 5675–5684.
Huai, B., Yang, Q., Qian, Y., Qian, W., Kang, Z., Liu, J., 2019. ABA-induced sugar transporter TaSTP6 promotes wheat susceptibility to stripe Rust1 OPEN. Plant Physiol. 181 (3), 1328–1343.
Humphrey, P.T., Whiteman, N.K., 2020. Insect herbivory reshapes a native leaf microbiome. Nat. Ecol. Evol. 4 (2), 221–229.
Igiehon, N.O., Babalola, O.O., 2017. Biofertilizers and sustainable agriculture: exploring arbuscular mycorrhizal fungi. Appl. Microbiol. Biotechnol. 101 (12), 4871–4881.
Jia, T., Wang, R.H., Fan, X.H., Chai, B.F., 2018. A comparative study of fungal community structure, diversity and richness between the soil and the phyllosphere of native grass species in a copper tailings dam in Shanxi Province, China. Appl. Sci. - Basel 8 (8), 1297.
Koljalg, U., Larsson, K.H., Abarenkov, K., Nilsson, R.H., Alexander, I.J., Eberhardt, U., Erland, S., Hoiland, K., Kjoller, R., Larsson, E., et al., 2005. UNITE: a database providing web-based methods for the molecular identification of ectomycorrhizal fungi. N. Phytol. 166 (3), 1063–1068.
Krämer, U.J.Aropb, 2010. Metal hyperaccumulation in plants. Annu. Rev. Plant Biol. 61 (1), 517–534.

Kumar, S., Stecher, G., Tamura, K., 2016. MEGA7: molecular evolutionary genetics analysis version 7.0 for bigger datasets. Mol. Biol. Evol. 33 (7), 1870–1874.
Langille, M.G.I., Zaneveld, J., Caporaso, J.G., McDonald, D., Knights, D., Reyes, J.A., Clemente, J.C., Burkepile, D.E., Thurber, R.L.V., Knight, R., et al., 2013. Predictive functional profiling of microbial communities using 16S rRNA marker gene sequences. Nat. Biotechnol. 31 (9), 814–821.
Letunic, I., Bork, P., 2011. Interactive Tree Of Life v2: online annotation and display of phylogenetic trees made easy. Nucleic Acids Res. 39, W475–W478.
Li, P.D., Zhu, Z.R., Zhang, Y.Z., Xu, J.P., Wang, H.K., Wang, Z.Y., Li, H.Y., 2022. The phyllosphere microbiome shifts toward combating melanose pathogen. Microbiome 10 (1), 1–17.
Liu, H.W., Brettell, L.E., Singh, B., 2020. Linking the phyllosphere microbiome to plant health. Trends Plant Sci. 25 (9), 841–844.
Lu, L.L., Tian, S.K., Yang, X.E., Wang, X.C., Brown, P., Li, T.Q., He, Z.L., 2008. Enhanced root-to-shoot translocation of cadmium in the hyperaccumulating ecotype of Sedum alfredii. J. Exp. Bot. 59 (11), 3203–3213.
Manara, A., Fasani, E., Furini, A., DalCorso, G., 2020. Evolution of the metal hyperaccumulation and hypertolerance traits. Plant Cell Environ. 43 (12), 2969–2986.
McGrath, S.P., Zhao, F.J., 2003. Phytoextraction of metals and metalloids from contaminated soils. Curr. Opin. Biotechnol. 14 (3), 277–282.
Mejia, L.C., Rojas, E.I., Maynard, Z., Van Bael, S., Arnold, A.E., Hebbar, P., Samuels, G.J., Robbins, N., Herre, E.A., 2008. Endophytic fungi as biocontrol agents of Theobroma cacao pathogens. Biol. Control 46 (1), 4–14.
Morina, F., Mijovilovich, A., Koloniuk, I., Pěnčík, A., Grúz, J., Novák, O., Küpper, H., 2021. Interactions between zinc and Phomopsis longicolla infection in roots of Glycine max. J. Exp. Bot. 72, 3320–3336.
Nerva, L., Pagliarani, C., Pugliese, M., Monchiero, M., Gonthier, S., Gullino, M.L., Gambino, G., Chitarra, W., 2019. Grapevine phyllosphere community analysis in response to elicitor application against powdery mildew. Microorganisms 7 (12), 662.
Nie, S.A., Lei, X.M., Zhao, L.X., Brookes, P.C., Wang, F., Chen, C.R., Yang, W.H., Xing, S. H., 2018. Fungal communities and functions response to long-term fertilization in paddy soils. Appl. Soil Ecol. 130, 251–258.
Quast, C., Pruesse, E., Yilmaz, P., Gerken, J., Schweer, T., Yarza, P., Peplies, J., Glockner, F.O., 2013. The SILVA ribosomal RNA gene database project: improved data processing and web-based tools. Nucleic Acids Res. 41 (D1), D590–D596.
Robinson, M.D., McCarthy, D.J., Smyth, G.K., 2010. edgeR: a Bioconductor package for differential expression analysis of digital gene expression data. Bioinformatics 26 (1), 139–140.
Rubina, K., Anjani, K., Nayak, A.K., Md, S., Rahul, T., Vijayakumar, S., Debarati, B., Upendra, K., Sangita, M., Panneerselvam, P., et al., 2020. Metal(loid)s (As, Hg, Se, Pb and Cd) in paddy soil: bioavailability and potential risk to human health. Sci. Total Environ. 699, 134330-134330.
Ruiz-Perez, C.A., Restrepo, S., Mercedes, Zambrano, M., 2016. Microbial and functional diversity within the phyllosphere of Espeletia species in an Andean high-mountain ecosystem. Appl. Environ. Microbiol. 82 (6), 1807–1817.
Salas-Gonzalez, I., Reyt, G., Flis, P., Custodio, V., Gopaulchan, D., Bakhoum, N., Dew, T. P., Suresh, K., Franke, R.B., Dangl, J.L., et al., 2021. Coordination between microbiota and root endodermis supports plant mineral nutrient homeostasis. Science 371 (6525), eabd0695.
Shi, Y., Delgado-Baquerizo, M., Li, Y., Yang, Y., Zhu, Y.-G., Penuelas, J., Chu, H., 2020. Abundance of kinless hubs within soil microbial networks are associated with high functional potential in agricultural ecosystems. Environ. Int. 142, 105869.
Stone, B.W.G., Weingarten, E.A., Jackson, C.R., 2018. The role of the phyllosphere microbiome in plant health and function. Annu. Plant Rev. Online 1 (2), 533–556.
Tangahu B.V., Sheikh Abdullah S.R., Basri H., Idris M., Anuar N., Mukhlisin M., 2011. A review on heavy metals (As, Pb, and Hg) uptake by plants through phytoremediation. International journal of chemical engineering 2011.
Tian, S., Lu, L., Labavitch, J., Yang, X., He, Z., Hu, H., Sarangi, R., Newville, M., Commisso, J., Brown, P., 2011. Cellular sequestration of cadmium in the hyperaccumulator plant species Sedum alfredii. Plant Physiol. 157 (4), 1914–1925.
Tian, S.K., Xie, R.H., Wang, H.X., Hu, Y., Hou, D.D., Liao, X.C., Brown, P.H., Yang, H.X., Lin, X.Y., Labavitch, J.M., et al., 2017. Uptake, sequestration and tolerance of cadmium at cellular levels in the hyperaccumulator plant species Sedum alfredii. J. Exp. Bot. 68 (9), 2387–2398.
Toju, H., Tanabe, A.S., Sato, H., 2018. Network hubs in root-associated fungal metacommunities. Microbiome 6 (1), 1–16.
Villanueva R.A.M., Chen Z.J. 2019. ggplot2: Elegant graphics for data analysis, 2nd edition. Measurement-Interdisciplinary Research and Perspectives 17(3): 160–167.
Vorholt, J.A., 2012. Microbial life in the phyllosphere. Nat. Rev. Microbiol. 10 (12), 828–840.
Wagg, C., Schlaeppi, K., Banerjee, S., Kuramae, E.E., van der Heijden, M.G.A., 2019. Fungal-bacterial diversity and microbiome complexity predict ecosystem functioning. Nat. Commun. 10 (1), 4841.
Wang, R.Z., Hou, D.D., Chen, J.Z., Li, J.H., Fu, Y.Y., Wang, S., Zheng, W., Lu, L.L., Tian, S. K., 2020. Distinct rhizobacterial functional assemblies assist two Sedum alfredii ecotypes to adopt different survival strategies under lead stress. Environ. Int. 143, 105912.
Wei, B.G., Yang, L.S., 2010. A review of heavy metal contaminations in urban soils, urban road dusts and agricultural soils from China. Microchem. J. 94 (2), 99–107.
Wood, J.L., Zhang, C., Mathews, E.R., Tang, C., Franks, A.E., 2016. Microbial community dynamics in the rhizosphere of a cadmium hyper-accumulator. Sci. Rep. 6, 36067.
Xiao, N., Zhou, A., Kempher, M.L., Zhou, B.Y., Shi, Z.J., Yuan, M., Guo, X., Wu, L., Ning, D., Van Nostrand, J., et al., 2022. Disentangling direct from indirect relationships in association networks. Proc. Natl. Acad. Sci. U. S. A. 119 (2) e2109995119.
Xiong, C., He, J.Z., Singh, B.K., Zhu, Y.G., Wang, J.T., Li, P.P., Zhang, Q.B., Han, L.L., Shen, J.P., Ge, A.H., et al., 2021a. Rare taxa maintain the stability of crop mycobiomes and ecosystem functions. Environ. Microbiol. 23 (4), 1907–1924.
Xiong, C., Zhu, Y.-G., Wang, J.-T., Singh, B., Han, L.-L., Shen, J.-P., Li, P.-P., Wang, G.-B., Wu, C.-F., Ge, A.-H., et al., 2021b. Host selection shapes crop microbiome assembly and network complexity. N. Phytol. 229 (2), 1091–1104.
Yang, X.E., Long, X.X., Ye, H.B., He, Z.L., Calvert, D.V., Stoffella, P.J., 2004. Cadmium tolerance and hyperaccumulation in a new Zn-hyperaccumulating plant species (Sedum alfredii Hance). Plant Soil 259 (1–2), 181–189.
Zacchini, M., Pietrini, F., Mugnozza, G.S., Iori, V., Pietrosanti, L., Massacci, A., 2009. Metal tolerance, accumulation and translocation in poplar and willow clones treated with cadmium in hydroponics. Water Air Soil Pollut. 197 (1–4), 23–34.
Zeng, H.Q., Hu, W., Liu, G.Y., Xu, H.R., Wei, Y.X., Zhang, J.C., Shi, H.T., 2022. Microbiome-wide association studies between phyllosphere microbiota and ionome highlight the beneficial symbiosis of Lactococcus lactis in alleviating aluminium in cassava. Plant Physiol. Biochem. 171, 66–74.
Zhang, Wen-Li, D, Yu, Miao-Miao, Z., Qi, S., 2014. Cadmium exposure and its health effects: a 19-year follow-up study of a polluted area in China. Sci. Total Environ. 470–471, 224–228.
Zhao, F.J., McGrath, S.P., 2009. Biofortification and phytoremediation. Curr. Opin. Plant Biol. 12 (3), 373–380.
Zhao, F.J., Ma, Y.B., Zhu, Y.G., Tang, Z., McGrath, S.P., 2015. Soil contamination in China: current status and mitigation strategies. Environ. Sci. Technol. 49 (2), 750–759.
Zou, S., Wang, H., Li, Y., Kong, Z., Tang, D.J.N.P., 2018. The NB-LRR gene Pm60 confers powdery mildew resistance in wheat. N. Phytol. 218 (1), 298–309.